Non-Data-Aided Approach to I/Q Mismatch Compensation in Low-IF Receivers

Gye-Tae Gil, *Member, IEEE*, Young-Doo Kim, *Member, IEEE*, and Yong H. Lee, *Senior Member, IEEE*

***Abstract*—A digital signal processing (DSP) technique is presented that can compensate for the in-phase/quadrature-phase (I/Q) mismatch in low-intermediate frequency (IF) receivers. In particular, a non-data-aided (NDA) I/Q mismatch estimator is derived by exploiting the statistical independence between desired and image signals. The proposed technique obtains two baseband signals (uncompensated desired and image signals) from a digital IF signal and processes them to estimate and compensate for the I/Q mismatch. The mean-square error (MSE) of the estimate is analyzed. Computer simulation results indicate that the proposed technique can outperform existing adaptive DSP techniques that are based on the use of blind signal separation algorithms. It is observed that the image rejection ratio (IRR) of the proposed technique decreases monotonically with the number of observed samples for estimation, while that of conventional methods exhibits some floor.**

***Index Terms*—Blind, compensation, I/Q mismatch, low-intermediate frequency (IF) receivers, non-data-aided (NDA) estimation.**

I. Introduction

A low-intermediate frequency (IF) architecture uses quadrature mixing to downconvert a radio frequency (RF) signal to an IF band, which in theory provides infinite attenuation of the image band and removes the need for analog image rejection filtering [1], [2]. This type of architecture has an advantage over direct conversion in terms of robustness against dc offset and flicker noise. Although a low-IF architecture is a promising approach to the goal of single-chip radio receivers, its performance can be severely degraded by insufficient image rejection due to the I/Q mismatch. One approach to overcome such a problem is compensation by digital signal processing (DSP). Offline techniques that measure the mismatching effect from test signals were proposed in [3]–[5], while more sophisticated adaptive DSP techniques that apply a blind signal separation algorithm to the mismatch compensation were introduced in [6], [7]. The adaptive techniques do not need any test signals and are thus preferable to the offline techniques. This is particularly true when the mismatch parameter is time varying.

In this paper, an alternative DSP technique is presented that can also measure the effect of the I/Q mismatch directly from the received signal, without generating test signals. Unlike the schemes in [6] and [7], which are basically adaptive filters, the proposed technique is based on the use of a non-data-aided (NDA) mismatch estimator, which is derived by exploiting the statistical independence between the desired and image signals.[1] It is shown that the proposed compensator, consisting of the I/Q mismatch estimator followed by an image suppressor, can outperform the existing adaptive DSP techniques. Throughout the paper, the I/Q mismatch is assumed to be frequency independent, which is valid for narrowband signals.

The remainder of this paper is organized as follows. Section II describes the signal model used in the current study. The proposed technique is derived in Section III, and its properties are analyzed in Section IV. In Section V, the advantages of the proposed scheme over the existing techniques are demonstrated through computer simulations considering both additive white Gaussian noise (AWGN) and Rayleigh fading channel environments. Section VI contains the conclusion.

II. Signal Model

The signal model considered in this paper is shown in Fig. 1 [7]. Assuming ideal filtering and no additive noise, the received RF signal $r_{\mathrm{RF}}(t)$ can be represented as

$$r_{RF}(t) = 2\mathrm{Re}\left\{s(t)e^{j2\pi f_C t}\right\} + 2\mathrm{Re}\left\{q(t)e^{j2\pi f_I t}\right\} \qquad (1)$$

where f_C is the carrier frequency of the desired signal, $f_I = f_C - 2(f_C - f_{\mathrm{LO}})$, is the center frequency of the image band f_{LO} is the local oscillator frequency, and $s(t)$ and $q(t)$ are the baseband equivalent expressions of the signals in the desired band and image band, respectively. Note that the signal model in (1) is reasonably valid even in a noisy environment because $s(t)$ and $q(t)$ can represent "signal plus noise" in their respective bands. A quadrature mixer is used to downconvert the RF signal to an IF band, which then suffers from an amplitude mismatch ϵ and phase mismatch θ. Here, the mismatch parameters ϵ and θ are assumed to be quasistatic and frequency independent so that they are constant over a data frame and over a frequency band under consideration. In addition, there is a frequency offset given by $\Delta f = (f_C - f_{LO}) - f_{\mathrm{IF}}$, where f_{IF} denotes the desired

[1]Data-aided I/Q mismatch estimators, which are mainly useful for direct conversion receivers, were derived in [8] and [9].

Manuscript received June 18, 2005; revised September 7, 2006. The associate editor who have coordinated the review of this paper and approved it for publication is Prof. Jaume Riba. This work was supported in part by the University Information Technology Research Center Program of the government of Korea. This paper was presented in part at the IEEE Vehicular Technology Conference, Milan, Italy, May 2004.

G.-T. Gil is with the Advanced Technology Laboratory, R&D Group, Korea Telecom, Junmindong, Yuseonggu, Daejeon, 305-811, Korea (e-mail: gategil@kt.co.kr).

Y.-D. Kim is with the Communication and Connectivity Laboratory, Samsung Advanced Institute of Technology, Gyeonggi, 446-712, Korea (e-mail: young-doo.kim@samsung.com).

Y. H. Lee is with the Department of Electrical Engineering and Computer Science, Korea Advanced Institute of Science and Technology, Daejeon, 305-701, Korea (e-mail: yohlee@ee.kaist.ac.kr).

Color versions of one or more of the figures in this paper are available online at http://ieeexplore.ieee.org.

Digital Object Identifier 10.1109/TSP.2007.893929

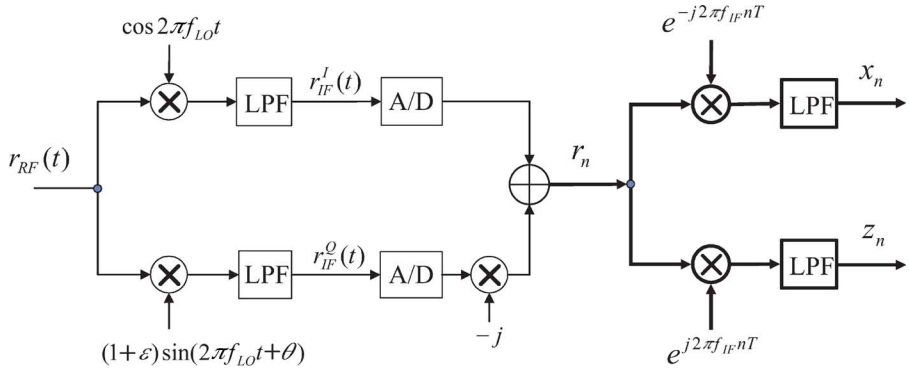

Fig. 1. Signal model. Complex-valued processing is illustrated in bold.

IF frequency. The analog IF band signals before analog-to-digital (A/D) conversion $r^I_{\rm IF}(t)$ and $r^Q_{\rm IF}(t)$ in Fig. 1, can be expressed as

$$r^I_{IF}(t) = \frac{1}{2}\left[s(t)+q^*(t)\right]e^{j2\pi(f_{IF}+\Delta f)t} + \frac{1}{2}\left[q(t)+s^*(t)\right]e^{-j2\pi(f_{IF}+\Delta f)t} \quad (2)$$

and

$$r^Q_{IF}(t) = \frac{1+\epsilon}{2j}\left[-s(t)e^{-j\theta}+q^*(t)e^{j\theta}\right]e^{j2\pi(f_{IF}+\Delta f)t} + \frac{1+\epsilon}{2j}\left[-q(t)e^{-j\theta}+s^*(t)e^{j\theta}\right]e^{-j2\pi(f_{IF}+\Delta f)t}. \quad (3)$$

The digital IF signal $\{r_n | n = 0, 1, \ldots, N-1\}$ after sampling at the rate of $1/T$ can be expressed as

$$r_n = \left(\beta_o s_n + \alpha_o q_n^*\right)e^{j2\pi(f_{IF}+\Delta f)nT} + \left(\beta_o q_n + \alpha_o s_n^*\right)e^{-j2\pi(f_{IF}+\Delta f)nT} \quad (4)$$

where $\beta_o = (1/2)[1 + (1+\epsilon)e^{-j\theta}]$, $\alpha_o = (1/2)[1 - (1+\epsilon)e^{j\theta}]$, $s_n = s(t)|_{t=nT}$, and $q_n = q(t)|_{t=nT}$. The two baseband signals $\{x_n\}$ and$\{z_n\}$ obtained by downconverting $\{r_n\}$ and then low-pass filtering in the digital domain are given by

$$x_n = \beta_o s_n e^{j2\pi n\nu} + \alpha_o (q_n e^{-j2\pi n\nu})^* \quad (5)$$

and

$$z_n = \beta_o q_n e^{-j2\pi n\nu} + \alpha_o (s_n e^{j2\pi n\nu})^* \quad (6)$$

where ν is the normalized frequency offset given by $\nu = \Delta f T$. If the downconversion circuit is free from the I/Q mismatch ($\epsilon = 0$ and $\theta = 0°$), then $\beta_o = 1$ and $\alpha_o = 0$. In this case, $x_n = s_n e^{j2\pi n\nu}$, and it is not necessary to generate z_n. The two signals $\{x_n\}$ and $\{z_n\}$ are needed for estimating the mismatch parameters β_o and α_o. When $\nu = 0$, the signal model in (5) and (6) becomes identical to the one in [7] and a special case of the model in [6] which considers a frequency dependent I/Q mismatch.

III. Proposed Technique

Given the baseband digital signals $\{x_n\}$ and $\{z_n\}$ in (5) and (6), the image signal can be suppressed by exploiting the following relation[2]:

$$x_n - \alpha z_n^* = \left(1 - |\alpha|^2\right)\beta_o s_n e^{j2\pi n\nu} \quad (7)$$

where $\alpha = \alpha_o/\beta_o^*$. The right-hand-side (RHS) of (7) represents the reconstructed signal in the desired band, which is a scaled version of $\{s_n e^{j2\pi n\nu}\}$. A dual equation of (7) can be written as

$$z_n - \alpha x_n^* = \left(1 - |\alpha|^2\right)\beta_o q_n e^{-j2\pi n\nu}. \quad (8)$$

Since the I/Q mismatch can be corrected once α is known (Fig. 2), the I/Q mismatch parameter estimation reduces to the estimation of α. A property of α that can be derived from the definitions of β_o and α_o in (4) can be stated as follows:

$$|\alpha| < 1 \quad \text{for } |\theta| < \pi/2. \quad (9)$$

Suppose that the desired and image signals $\{s_n\}$ and $\{q_n\}$ are zero-mean wide-sense stationary (WSS) random processes which are mutually uncorrelated. Then, from (7) and (8)

$$E\left[(x_n - \alpha z_n^*)(z_n - \alpha x_n^*)\right] = \left(1 - |\alpha|^2\right)^2 \beta_o^2 E[s_n q_n] = 0. \quad (10)$$

Solving (10) for α results in

$$\alpha = \frac{b \pm \sqrt{b^2 - 4|c|^2}}{2c^*} \quad (11)$$

where $b = E[|x_n|^2 + |z_n|^2]$ and $c = E[x_n z_n]$. Using the Cauchy–Schwartz inequality, it is straightforward to show that $b^2 - 4|c|^2 \geq 0$. In (10), let $\alpha_1 = (b - \sqrt{b^2 - 4|c|^2})/2c^*$ and $\alpha_2 = (b + \sqrt{b^2 - 4|c|^2})/2c^*$. Then, $\alpha_2 = 1/\alpha_1^*$ and $|\alpha_1| \leq |\alpha_2|$. These facts indicate that $|\alpha_1| \leq 1$ and $|\alpha_2| \geq 1$. From (9) and the fact that $|\theta| \ll \pi/2$ in practice, we discard α_2

[2]If $\{s_n\}$ is a training sequence corrupted by an additive white Gaussian noise (data-aided case), then the maximum-likelihood estimation of α can be derived from (7) following the approach in [9].

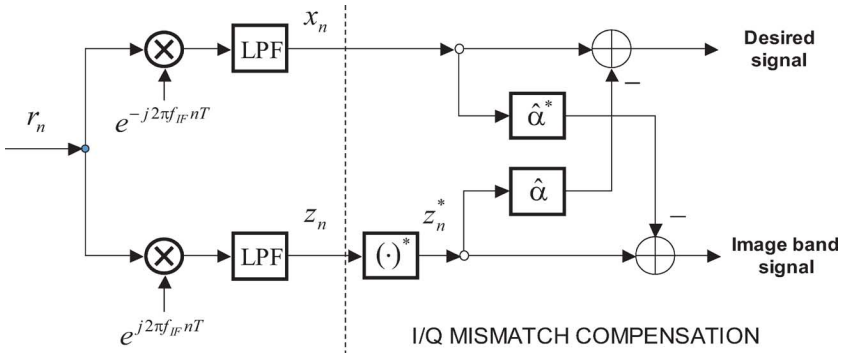

Fig. 2. I/Q mismatch compensation structure. Here, $\hat{\alpha}$ is an estimate of α.

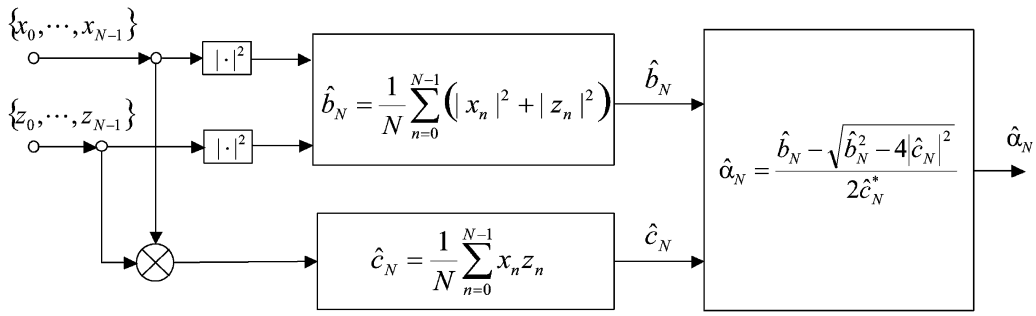

Fig. 3. Proposed estimator.

and use α_1 to estimate α. Specifically, the estimate of α is given by

$$\hat{\alpha}_N = \frac{\hat{b}_N - \sqrt{\hat{b}_N^2 - 4|\hat{c}_N|^2}}{2\hat{c}_N^*} \tag{12}$$

where $\hat{b}_N$ and $\hat{c}_N$ are the sample means given by $\hat{b}_N = (1/N)\sum_{n=0}^{N-1}(|x_n|^2 + |z_n|^2)$ and $\hat{c}_N = (1/N)\sum_{n=0}^{N-1} x_n z_n$. The block diagram of the proposed estimate in (12) is shown in Fig. 3.

IV. Performance Analysis

To find the mean and mean-square error (MSE) of $\hat{\alpha}_N$ as $N \to \infty$, we use the first-order Taylor series expansion of $\hat{\alpha}_N$ around b, c_I and c_Q, where c_I and c_Q represent the real and imaginary parts of c, respectively. If $\{s_n\}$ and $\{q_n\}$ are independent identically distributed (i.i.d.), then, as shown in Appendix A, $\hat{\alpha}_N$ in (12) can be linearized as

$$\hat{\alpha}_N = \alpha + \frac{\left(|\beta_o|^2 - |\alpha_o|^2\right)}{\beta_o^{*2}\left(\sigma_s^2+\sigma_q^2\right)}\frac{1}{N}\sum_{n=0}^{N-1} s_n q_n + o_P(1/\sqrt{N}) \tag{13}$$

where $\sigma_s^2 = E[|s_n|^2]$, $\sigma_q^2 = E[|q_n|^2]$, and $o_P(1/\sqrt{N})$ indicates that $\sqrt{N}$ times the remainder converges to zero in probability as $N \to \infty$ [13]. Reference (13) can be rewritten as

$$\sqrt{N}(\hat{\alpha}_N - \alpha) = \frac{\left(|\beta_o|^2 - |\alpha_o|^2\right)}{\beta_o^{*2}\left(\sigma_s^2+\sigma_q^2\right)}\frac{1}{\sqrt{N}}\sum_{n=0}^{N-1} s_n q_n + o_P(1). \tag{14}$$

Since $\{s_n\}$ and $\{q_n\}$ are i.i.d. and mutually uncorrelated, it follows from the central limit theorem [14] that the first term in the RHS of (14) converges in distribution to a random variable ξ which is zero-mean complex Gaussian with variance

$$\left|\frac{\left(|\beta_o|^2 - |\alpha_o|^2\right)}{\beta_o^{*2}\left(\sigma_s^2+\sigma_q^2\right)}\right|^2 \sigma_s^2\sigma_q^2 = \frac{\left(1-|\alpha|^2\right)^2\sigma_s^2\sigma_q^2}{\left(\sigma_s^2+\sigma_q^2\right)^2}. \tag{15}$$

Then, $\sqrt{N}(\hat{\alpha}_N - \alpha)$ in (14) also converges in distribution to ξ [13, p. 424]. Therefore, $\hat{\alpha}_N$ is asymptotically unbiased and its asymptotic variance is given by $1/N$ times the term in (15), which is rewritten as

$$E\left[|\hat{\alpha}_N - \alpha|^2\right] = \frac{\left(1-|\alpha|^2\right)^2}{N}\frac{1}{\rho + 2 + 1/\rho}$$

where ρ is the signal-to-image ratio (SIR) defined as $\rho = \sigma_s^2/\sigma_q^2$. It is interesting to note that the MSEs corresponding to ρ and $1/\rho$ are identical. This occurs because of the duality between x_n in (5) and z_n in (6). Given N and α, the MSE is upper bounded by $(1-|\alpha|)^2/(4N)$ which is the MSE for $\rho = 1$ (input SIR = 0 dB) and decreases monotonically with N and $\rho(1/\rho)$ when $\rho > 1(\rho < 1)$.

V. Simulation

The performance of the proposed estimator was examined through computer simulations. The baseband equivalent signals in the desired and image bands are expressed by $s_n = \sum_{l=0}^{L-1} h_n^l a_{n-l} + w_n$ and $q_n = \sum_{l=0}^{L-1} g_n^l b_{n-l} + \eta_n$, respectively, where $\{a_n\}$ and $\{b_n\}$ are the transmitted symbols that are quadrature phase-shift keying (QPSK), $\{h_n^l | l = 0,1,\cdots,L-1\}$ and $\{g_n^l | l = 0,1,\cdots,L-1\}$ denote the channel responses at time n, and $\{w_n\}$ and $\{\eta_n\}$ denote AWGN. The signal-to-noise ratios (SNRs) of the received signals $\{s_n\}$ and $\{q_n\}$ were 20 dB.

TABLE I
COMPUTATIONAL LOAD REQUIRED FOR PROCESSING N SAMPLES

Algorithm	Real products	Real additions
proposed	$8N+8$	$8N$
method in [6]	$20N-12$	$16N-8$
method in [7]	$96N$	$80N$

Two types of channels were considered: AWGN channels ($L=1, h_n^0=g_n^0=1$) and Rayleigh fading channels with eight paths ($L=8$) that had an identical average power and $f_DT=0.01$, where f_D is the maximum Doppler frequency. Jakes' model was used for generating the channel parameters [10]. The frequency offset $\nu=0.01$. The amplitude mismatch $\epsilon=0.1$ and phase mismatch $\theta=10^\circ$ ($\alpha_o=-0.0416-j0.0955$, $\beta_o=1.0416-j0.0955$, and $\alpha=-0.048-j0.0873$). The input SIR $\rho\in\{0,\pm10,\pm20,\pm30\}$ dB. In the simulation, the MSE and image rejection ratio (IRR) [11], which is the ratio between the input SIR ρ and the SIR of $x_n-\hat{\alpha}_N z_n^*$, were empirically estimated based on 100 trials. The MSEs in AWGN channels were evaluated for the proposed estimator to confirm the analytical results in Section IV. Those with different A/D resolutions were also evaluated in order to examine the impact of finite word length. The proposed algorithm was compared with the existing methods in [6] and [7], which are summarized below, in terms of the IRR and computational complexity.

Method in [6]: The filtering and weight update equations are represented as $\hat{s}_n=x_n-w_n^{(1)}z_n$ and $\hat{q}_n=z_n-w_n^{(2)}x_n$, where the weights are updated by $w_{n+1}^{(1)}=w_n^{(1)}+\mu\hat{q}_n\hat{s}_n^*$ and $w_{n+1}^{(2)}=w_n^{(2)}+\mu\hat{s}_n\hat{q}_n^*$. Note that this method employs single-tap adaptive filters for the frequency independent I/Q mismatch. It recursively estimates the mismatch parameter α in (7) by updating the weight $w_n^{(1)}$. The step size μ was set at 0.0001, which was chosen to reduce the steady-state error, while guaranteeing the convergence within 10 000 iterations.

Method in [7]: This is called the *equivariant adaptive separation via independence (EASI)* algorithm. The estimate of $\{s_n,q_n\}$ is denoted by $\mathbf{y}_n=[y_n^{(1)},y_n^{(2)}]^T$, in which some additional information is needed to determine whether $\hat{s}_n=y_n^{(1)}$ or $\hat{s}_n=y_n^{(2)}$. The vector $\mathbf{y}_n$ is represented as $\mathbf{y}_n=\mathbf{B}_n[x_n,z_n^*]^T$, where $\mathbf{B}_n$ is the 2×2 separating matrix, which is updated by $\mathbf{B}_{n+1}=\mathbf{B}_n-\mu G(\mathbf{y}_n)\mathbf{B}_n$. Here, $G(\mathbf{y}_n)=\mathbf{y}_n\mathbf{y}_n^H-\mathbf{I}+f(\mathbf{y}_n)\mathbf{y}_n^H-\mathbf{y}_n f(\mathbf{y}_n)^H$, and $f(\mathbf{y}_n)$ is the 2×1 vector whose ith element is given by $y_n^{(i)}|y_n^{(i)}|^2$. The stepsize μ and the initial separating matrix $\mathbf{B}_0$ were determined as in [7]. For the Rayleigh fading channel, the normalized EASI algorithm in [12] was used to track the time variation of the channel.

The computational complexities required for processing N data samples are compared in Table I. The proposed method is simpler to implement than the existing methods when $N\geq2$.

Fig. 4 shows the MSEs obtained from the analysis and simulation for the AWGN channels. A remarkably good agreement was observed between the analytical and simulation results. As expected, the MSE decreased monotonically with N and $\rho(1/\rho)$ when $\rho>1(\rho<1)$.

Fig. 5 shows the MSE performance of the proposed estimator versus A/D converter resolution for AWGN channels

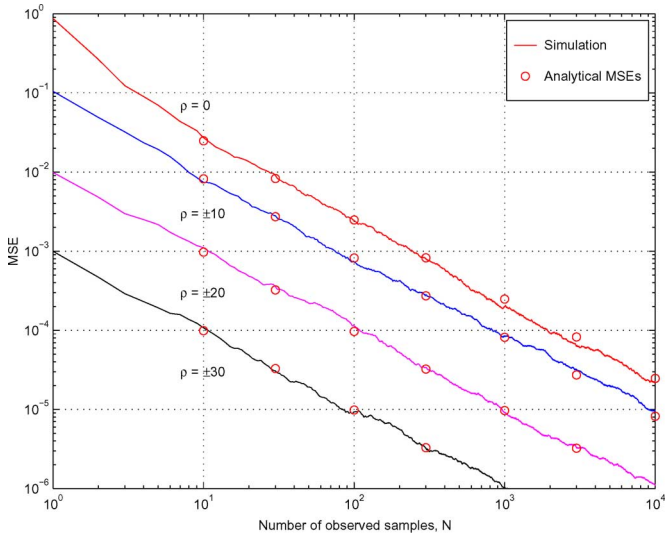

Fig. 4. MSE performance of proposed estimator for AWGN channels.

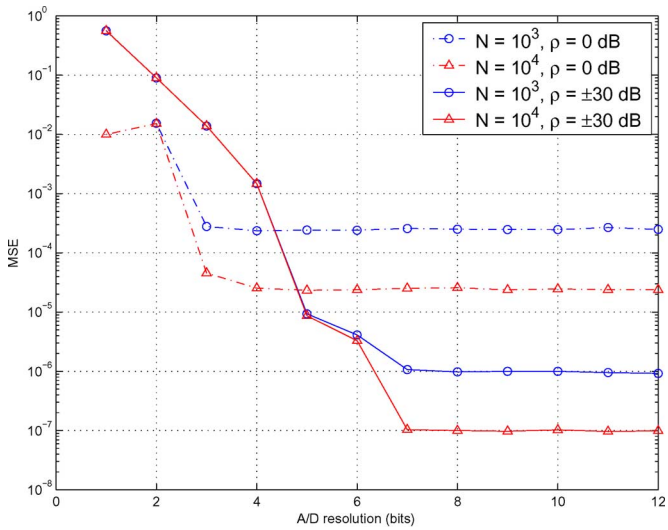

Fig. 5. MSE variation of proposed estimator with A/D converter resolution for AWGN channels.

when $N=1000$ and 10 000. The MSEs were evaluated for $\rho\in\{0,\pm30\}$ dB. The A/D converter resolution required by the proposed estimator was low: only 4-bit was needed for $\rho=0$ dB and 7-bit for $\rho=\pm30$ dB. The required resolution increases with $\rho(1/\rho)$ because the MSE decreases as $\rho(1/\rho)$ increases when $\rho>1(\rho<1)$.

Figs. 6 and 7 show the IRRs for the AWGN and Rayleigh fading channels, respectively. Comparing the IRR curves indicates that neither technique was vulnerable to the channel type: the IRR curves for the AWGN channels were similar to the corresponding IRR curves for the Rayleigh fading channels. The proposed method outperformed the methods in [6] and [7] when the number of observed samples N was greater than or equal to 11. Furthermore, the IRR of the former decreased monotonically with N, while the IRR curves of the latter exhibited some floor.

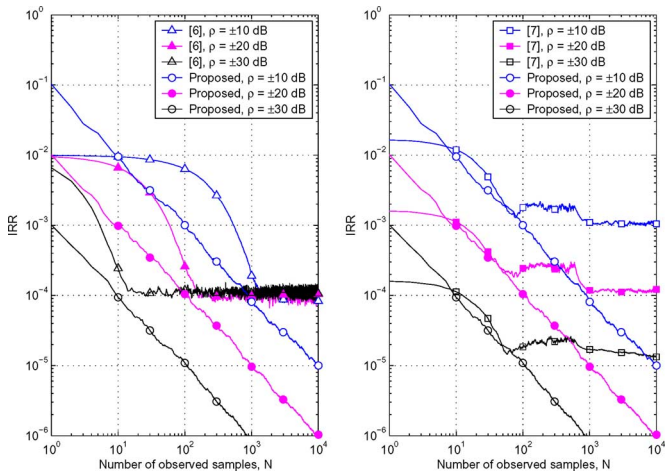

Fig. 6. IRR performances for AWGN channels.

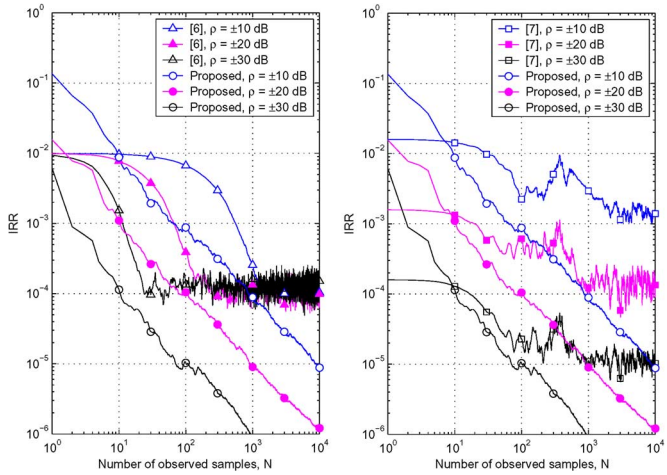

Fig. 7. IRR performances for frequency-selective fading channels.

VI. Conclusion

In this paper, an NDA I/Q mismatch estimator for low-IF receivers was developed and applied to I/Q mismatch compensation. Numerical simulations indicate that the MSE of the proposed estimator and IRR of the resulting compensator decreased monotonically with the number of observed samples, while the IRR curves of an existing adaptive technique exhibited some floor. In contrast to the adaptive techniques in [6] and [7], both of which require some caution to guarantee convergence of the algorithm, the proposed technique is free from convergence issues. This is because the proposed estimator is a batch processor in which all data are collected together and processed simultaneously. The proposed method can track time-varying mismatch effects in the sense that it can compensate for quasi-static mismatches that may vary from one frame to another. Finally, it should be pointed out that the use of the proposed scheme is limited to the case of frequency independent mismatches, while the adaptive technique in [6] can be applicable to frequency dependent situations.

Appendix A

To prove (13), we first show that $\hat{b}_N - b = O_P(1/\sqrt{N})$ and $\hat{c}_N - c = O_P(1/\sqrt{N})$, where $O_P(1/\sqrt{N})$ indicates that $\sqrt{N}(\hat{b}_N - b)$ and $\sqrt{N}(\hat{c}_N - c)$ are bounded in probability [13]. From the central limit theorem, it can be shown that [13, p. 425]

$$\frac{1}{N}\sum_{n=0}^{N-1} s_n q_n = O_P(1/\sqrt{N}) \tag{A1}$$

and

$$\frac{1}{N}\sum_{n=0}^{N-1} \left(|s_n|^2 + |q_n|^2\right) = \sigma_s^2 + \sigma_q^2 + O_P(1/\sqrt{N}). \tag{A2}$$

Now $\hat{b}_N$, $\hat{c}_N$, b, and c can be rewritten as

$$\begin{aligned}\hat{b}_N = &\frac{1}{N}\sum_{n=0}^{N-1}\left[\left(|\beta_o|^2 + |\alpha_o|^2\right)\left(|s_n|^2 + |q_n|^2\right)\right] \\ &+ \frac{1}{N}\sum_{n=0}^{N-1}\left[2\alpha_o^*\beta_o s_n q_n + 2\alpha_o\beta_o^* s_n^* q_n^*\right] \end{aligned}\tag{A3}$$

$$\begin{aligned}\hat{c}_N = &\frac{1}{N}\sum_{n=0}^{N-1}\left[\beta_o\alpha_o\left(|s_n|^2 + |q_n|^2\right)\right] \\ &+ \frac{1}{N}\sum_{n=0}^{N-1}\left[\beta_o^2 s_n q_n + \alpha_o^2 s_n^* q_n^*\right] \end{aligned}\tag{A4}$$

$$b = \left(|\beta_o|^2 + |\alpha_o|^2\right)\left(\sigma_s^2 + \sigma_q^2\right) \tag{A5}$$

and

$$c = \beta_o\alpha_o\left(\sigma_s^2 + \sigma_q^2\right). \tag{A6}$$

The boundedness of $\sqrt{N}(\hat{b}_N - b)$ and $\sqrt{N}(\hat{c}_N - c)$ in probability can be proved by using (A1) and (A2) in (A3)–(A6). Taking the Taylor series expansion of $\hat{\alpha}_N$ to the first-order terms around b, c_I and c_Q gives

$$\begin{aligned}&\hat{\alpha}_N(\hat{b}_N, \hat{c}_{N,I}, \hat{c}_{N,Q}) \\ &\quad= \alpha + \left.\frac{\partial\hat{\alpha}_N}{\partial\hat{b}_N}\right|_{\hat{b}_N=b,\hat{c}_{N,I}=c_I,\hat{c}_{N,Q}=c_Q}(\hat{b}_N - b) \\ &\qquad+ \left.\frac{\partial\hat{\alpha}_N}{\partial\hat{c}_{N,I}}\right|_{\hat{b}_N=b,\hat{c}_{N,I}=c_I,\hat{c}_{N,Q}=c_Q}(\hat{c}_{N,I} - c_I) \\ &\qquad+ \left.\frac{\partial\hat{\alpha}_N}{\partial\hat{c}_{N,Q}}\right|_{\hat{b}_N=b,\hat{c}_{N,I}=c_I,\hat{c}_{N,Q}=c_Q}(\hat{c}_{N,Q} - c_Q) \\ &\qquad+ o_P(1/\sqrt{N})\end{aligned}\tag{A7}$$

where $\hat{c}_{N,I}$ and $\hat{c}_{N,Q}$ denote the real and imaginary parts of $\hat{c}_N$, respectively. In (A7), $o_P(1/\sqrt{N})$ follows from the facts that $\hat{b}_N = b + O_P(1/\sqrt{N})$ and $\hat{c}_N = c + O_P(1/\sqrt{N})$ [13, p. 423]. By evaluating the derivatives in (A7), we can get the expression of $\hat{\alpha}_N$ in (13).

Acknowledgment

The authors would like to thank the anonymous reviewers whose constructive comments have improved the quality of this paper.

REFERENCES

[1] J. Crols and M. S. J. Steyaert, "Low-IF topologies for high-performance analog front ends of fully integrated receivers," *IEEE Trans. Circuits Syst.*, vol. 45, pp. 269–282, Mar. 1998.

[2] S. Mirabbasi and K. Martin, "Classical and modern receiver architectures," *IEEE Commun. Mag.*, vol. 38, pp. 132–139, Nov. 2000.

[3] F. E. Churchill, G. W. Ogar, and B. J. Thomson, "The correction of I and Q errors in a coherent processor," *IEEE Trans. Aerosp. Electron. Sys.*, vol. 17, pp. 131–137, Jan. 1981.

[4] R. A. Green, R. Anderson-Sprecher, and J. W. Pierre, "Quadrature receiver mismatch calibration," *IEEE Trans. Signal Process.*, vol. 47, no. 11, pp. 3130–3133, Nov. 1999.

[5] C. C. Chen and C. C. Huang, "On the architecture and performance of a hybrid image rejection receiver," *IEEE J. Sel. Areas Commun.*, vol. 19, pp. 1029–1040, Jun. 2001.

[6] L. Yu and W. M. Snelgrove, "A novel adaptive mismatch cancellation system for quadrature IF radio receivers," *IEEE Trans. Circuits Syst. II*, vol. 46, pp. 789–801, Jun. 1999.

[7] M. Valkama, M. Renfors, and V. Koivunen, "Advanced methods for I/Q imbalance compensation in communication receivers," *IEEE Trans. Signal Process.*, vol. 49, no. 10, pp. 2335–2344, Oct. 2001.

[8] I. H. Sohn, E. R. Jeong, and Y. H. Lee, "Data-aided approach to I/Q mismatch and DC offset compensation in communication receivers," *IEEE Commun. Lett.*, vol. 6, pp. 547–549, Dec. 2002.

[9] G. T. Gil, I. H. Sohn, J. K. Park, and Y. H. Lee, "Joint ML estimation of carrier frequency, channel, I/Q mismatch, and DC offset in communication receivers," *IEEE Trans. Veh. Technol.*, vol. 54, pp. 338–349, Jan. 2005.

[10] W. C. Jakes, *Microwave Mobile Communications*. New York: Wiley, 1974.

[11] B. Razavi, *RF Microelectronics*. Englewood Cliffs, NJ: Prentice-Hall, 1998.

[12] J. F. Cardoso and B. H. Laheld, "Equivariant adaptive source separation," *IEEE Trans. Signal Process.*, vol. 44, no. 12, pp. 3017–3030, Dec. 1996.

[13] B. Porat, *Digital Processing of Random Signals: Theory and Methods*. Englewood Cliffs, NJ: Prentice-Hall, 1994.

[14] P. Billingsley, *Probability and Measure*, 3rd ed. New York: Wiley, 1995.

Gye-Tae Gil (M'04) was born in Daejeon, Korea, on July 24, 1966. He received the B.S. degree in electronic communication engineering from Hanyang University, Seoul, Korea, in 1989 and the M.S. and Ph.D. degrees in electrical engineering from KAIST, Korea, in 1992 and 2004, respectively.

Since 1991, he has been with the research center of Korea Telecom, Daejeon, Korea, where he is currently a Principal Researcher. His research interests are in the area of communication signal processing, which includes synchronization, interference cancellation, and adaptive filter design for wireless communication systems. He is also interested in resource allocation for cellular orthogonal frequency-division multiple-access (OFDMA) systems.

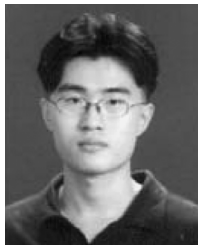

Young-Doo Kim (S'99–M'06) received the B.S., M.S., and Ph.D. degrees in electrical engineering from Korea Advanced Institute of Science and Technology (KAIST), Daejeon, Korea, in 1999, 2001, and 2006, respectively.

He has been with the Samsung Advanced Institute of Technology (SAIT), Gyeonggi-Do, Korea, since 2006. His primary research interests include synchronization, detection and estimation for communication systems, and predistortion linearization of nonlinear power amplifiers for wireless applications. Currently, he is focusing on the radio resource management in multihop and relaying networks.

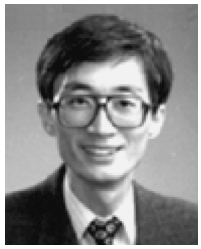

Yong H. Lee (SM'99) was born in Seoul, Korea, on July 12, 1955. He received the B.S. and M.S. degrees in electrical engineering from Seoul National University, Seoul, Korea, in 1978 and 1980, respectively, and the Ph.D. degree in electrical engineering from the University of Pennsylvania, Philadelphia, in 1984.

From 1984 to 1988, he was an Assistant Professor with the Department of Electrical and Computer Engineering, State University of New York, Buffalo. Since 1989, he has been with the Department of Electrical Engineering and Computer Science, Korea Advanced Institute of Science and Technology, Daejeon, Korea, where he currently is a Professor and the Dean of College of Engineering. His research activities are in the area of communication signal processing, which includes synchronization, estimation, detection, interference cancellation, and efficient filter design for code-division multiple access (CDMA), time-division multiple access (TDMA), and orthogonal frequency-division multiplexing systems. He is also interested in designing and implementing transceivers.